*EVS24*
*Stavanger, Norway, May 13-16, 2009*

# Design Methodology of Energy Storage Systems for a Small Electric Vehicle

João P. Trovão[1,3], Paulo G. Pereirinha[1,3,4], Humberto M. Jorge[2,3]
[1] *IPC-ISEC, Polytechnic Institute of Coimbra, Rua Pedro Nunes, Coimbra, Portugal, {jtrovao, ppereiri}@isec.pt*
[2] *DEEC – FCTUC, University of Coimbra - Pólo II, P-3030-290 Coimbra, Portugal, hjorge@deec.uc.pt*
[3] *INESC-Coimbra, Institute for Systems and Computers Engineering at Coimbra, Portugal*
[4] *APVE, Portuguese Electric Vehicle Association Portuguese Branch of AVERE, Lisboa, Portugal*

## Abstract

With the current state of technological development, the future of Electric Vehicles (EVs) seems to go through the hybridization of various Energy Storage Systems (ESSs). This strategy seeks to benefit from the best qualities of each available energy source, and is especially useful in urban driving. In this work, the need for multiple energy sources hybridization is addressed. A methodology to optimize the sizing of the ESSs for an electric vehicle taking as example the ISEC-VEIL project, using different driving cycles, maximum speed, a specified acceleration, energy regeneration and gradeability requests are presented. It is also studied the possibility of using a backup system based on solar energy, that may be considered in the design, or as an extra to cope with unforeseen routines and to minimize the recharge of ESSs. Some simulation results of multiple energy sources hybridization are presented, considering different ESSs and different scenarios for the small presented EV, in order to verify the proposed designs.

*Keywords: Neighborhood Electric vehicle (NEV), optimization, energy storages, battery electric vehicle (BEV), cost reduction.*

## 1 Introduction

The energy supply problem, with economic, ecologic and geopolitical aspects, is at the heart of today's political and scientific agenda. In 2005, the transports sector accounted for 60.3% of world oil consumption, against 45.4% in 1973 [1][2]. This increasingly fuel consumption leads to forecast oil shortage and price rise, confirmed by the July 2008 crude oil spot prices, very close to US$150. Even if the present world economic crisis releases, for the moment, some of the price problem, there are also very important energy dependence and security concerns as the crude oil come mainly from middle east and/or instable countries.

The mass utilization of Internal Combustion Engine (ICE) vehicles in the transportation sector also increases pollution emissions, especially Greenhouse Gas emissions, which must be prevented for the sustainability of the planet and for life quality.

Concerning urban pollution, the emissions of ICE vehicles are one of its major sources, especially in medium and large cities. The high incidence of respiratory problems, allergies, asthmas, and some cancers is an increasing problem, leading to public health concerns, as air pollution contributes definitively to mortality and morbidity [3][4].

Due to its very high efficiency, no local emissions, silent driving, and its ability to recover breaking energy, electric machines are the key components to sustainable mobility and world's future, both in pure EVs or in HEVs. A transition step while looking forward the ideal solution of Zero Emissions

Vehicles, are the Low Emissions Vehicles, as the HEVs, specially the Plug-In HEVs (PHEVs) [5][6].

# 2 Energy Storage Systems for EVs

## 2.1 The Energy Storage Issue in EVs

To allow EV to become the effective sustainable transportation solution, a great effort has to be done in R&D to overcome the major technical issue in EVs: the energy storage.

Typically, an EV stores energy in batteries (Lead-Acid, NiMH or Li-Ion, for instance) that are bulky, heavy and expensive. The specific energy, in Wh/kg, of gasoline is about 12500 Wh/kg (which only 2000-3000 can be considered useful energy, due to the very low efficiency of the ICE) against typically 35 in good lead-acid batteries or 60 in NiMH, which gives an idea of the volume and weight necessary to store the energy needed to do the same work. Li-ion batteries have higher specific energy, usually from 80 to 120 Wh/kg, but they still quite expensive and have some safety issues that have to be carefully addressed. Due to this problem, with current batteries technologies it is very difficult to make a general purpose EV that effectively competes with ICE cars. For massive deployment of EV its driving range problem must be solved.

## 2.2 Main Available Energy Storage Systems

At the present and in the foreseeable future, the viable EVs energy sources seem to be batteries, fuel cells, supercapacitors (SCs) and ultrahigh-speed flywheels.

Batteries are the most mature source for EV application. But they offer either high specific energy (HSE) or (relatively) high specific power (HSP). Fuel cells are comparatively less mature and expensive for EV application. They can offer exceptionally HSE, but with very low specific power. In spite of some quite expensive prototypes, such low specific power poses serious problems to their application to EVs that desire a high acceleration rate or high hill climbing capability. Also, they are incapable of accepting the high peaks of regenerative energy during EV braking or downhill driving and, worse, their overall energy efficiency is very low (about 25% from "wind to wheel"). SCs have low specific energy for stand alone application. However, they can offer exceptionally HSP (with low specific energy). Flywheels are technologically immature for EV application.

For the "full electric" EV the solutions pass by significant progresses in battery technology and by using different energy sources with optimized management of energy flow. [9] [10]

## 2.3 Multiple Energy Sources Hybridization

As mentioned before, none of the available energy sources can easily fulfil alone all the demand of EVs to enable them to compete with gasoline powered vehicles. In essence, these energy sources have a common problem: they have either HSE or HSP, but not both. A HSE energy source is favourable for long driving range, whereas a HSP energy source is desirable for high acceleration rate and high hill climbing capability. The concept of using and coordinate multiple energy sources to power the EV is typically denominated *hybridization*. Hence, the specific advantages of the various EV energy sources can be fully utilized, leading to optimized fuel economy while satisfying the expected driving range and maintaining other EV performances. [10][11]

A lot of work has been done to investigate methodologies to sizing and control strategies for fuel-cell-battery [13], fuel-cell-supercapacitor [11], fuel-cell-battery-supercapacitor [10][13], battery-supercapacitor [12] vehicles. These studies add a significant knowledge to the field but do not provide a detailed comparison of a battery-supercapacitor-PV array, principally of the daily energy evolution, in function of the test cycle. As the fuel-cell vehicle is an expensive choice, it is necessary to analyze other solution for EV hybridization.

The present study aims at developing a methodology to help the designers to optimise the sizing of the power components in a small urban EV. For that, it used different driving cycles, specified acceleration performance and maximum speed requests.

# 3 Veil Prototype: Hybridization of Energy Storage Systems

At the Electrical Engineering Department of the Engineering Institute of Coimbra (DEE-ISEC) the author's team has started the on going VEIL project to convert a small vehicle, initially with an ICE, into an electric vehicle (Figure 1) [7][8][15].

For VEIL project prototype, it was considered to be viable the hybridization of three energy sources: a HSE storage system – Batteries –, a HSP system – SCs – and photovoltaic panels, PV. Figure 2 shows this hybridization configuration. [7] [8]


Figure 1: VEIL project in preparation at ISEC campus.

# 4 Design Methodology

The considered configuration of the VEIL powertrain consists of a battery bank, a supercapacitor bank, a photovoltaic panels array, a DC/DC converter, an inverter, an AC motor, and a transmission.

The multiple power converter regulates the VFD DC-link voltage and adapts the different voltage level of the considered Energy Storage Systems (ESSs). The VFD inverter converts the regulated DC voltage to an AC voltage to drive the AC motor. The transmission is a gearbox that increases the motor torque using a fixed gear reduction.

When the EV demands high power, the batteries and SCs provides power to the vehicle's wheels through the DC/DC converter, the inverter, AC motor, and the transmission. On the other hand, when the EV demands low power, the batteries provides power to the wheels through the DC/DC converter, the inverter, the AC motor, and the transmission and charges the SCs through the reversible DC/DC converter. When the vehicle brakes, the AC motor converts the kinetic energy of the vehicle into electricity and charges principally the SCs and residually the batteries through the inverter and the DC/DC converter

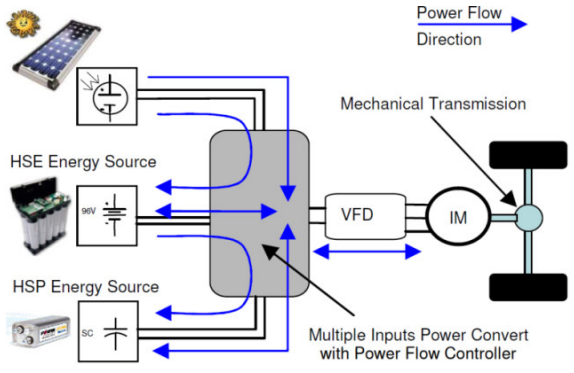


Figure 2: EV project power scheme.

using the generated energy. The solar panels array works as an energy back-up, as, whenever solar energy exists, the panels generate energy that is used by the system. In the tractive mode, this assists the stored energy and when the vehicle is parked, it provides a charge of the storage systems.

The power generated and stored in the energy system ($P_{st}$) at any time should be at least equal to EV power demand ($P_{dem}$).

$$P_{st} \geq P_{dem} \quad (1)$$

$P_{st}$ is composed by the batteries power ($P_{Bat}$), the SC power ($P_{SC}$), the PV array power ($P_{pv}$) and the regenerative break power ($P_{reg}$):

$$P_{st} = P_{Bat} + P_{SC} + P_{pv} + P_{reg} \quad (2)$$

On the other hand, the PV array has not a response capability for a high power request and should be seen as a backup system in order to recharge the batteries for a prolonged use, for daily journey and for extended parking periods, and for covering its self discharge. With this consideration, (2) can be simplified to (3), and the PV array energy complement is analyzed separately of the other ESSs.

$$P_{st} = P_{Bat} + P_{SC} + P_{reg} \quad (3)$$

The proposed methodology is based on the combination of ESSs with the lowest cost and weight, minimizing the number of storage units in series and parallel, maximizing autonomy and with a relatively better performance.

For the considered hybridization, the three energy devices can be divided into two types: a classic type (batteries and SCs), because, traditionally, the EVs use only batteries or more recently batteries and SCs, and a special type, as it is not common the EVs to use photovoltaic panels. Therefore, the design methodology needs to divide into a classic energy storage design and a backup energy supply design.

## 4.1 Classic Energy Storage Design

The design is based on the estimated power demand required by the EV powertrain, so that the EV makes a particular speed profile trip, responding to requests of drive cycles, for maximum speed, acceleration, breaking and gradeability.

The layout of the batteries bank and that of the SCs bank is shown in Figure 3. The battery and supercapacitor units are connected in series to form a branch and multiple branches are paralleled to form a battery bank and SC bank. Therefore, the total cost ($C_{Tc}$) of the ESSs is given by the sum of the unit cost ($C_{Bat}$ and $C_{SC}$) of the number of the series units ($X_{Bat}$ and $X_{SC}$) and parallel branches

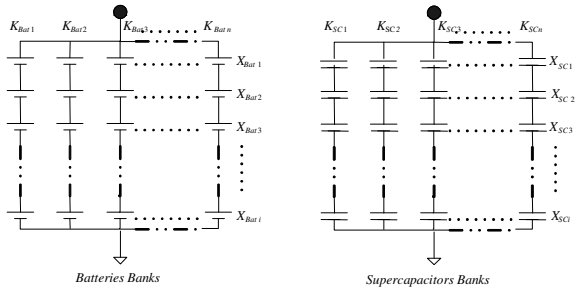


Figure 3: Layout of the Batteries and Supercapacitors Banks.

($K_{Bat}$ and $K_{SC}$) of the batteries and SCs, as presented in (4). The costs $C_{Tc}$, $C_{Bat}$, and $C_{SC}$ are in European Currency (Euro, €).

$$C_{T_c} = C_{Bat} \cdot X_{Bat_i} \cdot K_{Bat_n} + C_{SC} \cdot X_{SC_i} \cdot K_{SC_n} \quad (4)$$

The unit cost and specific characteristics of the samples battery units and SCs cells used in this work are presented in Table I. The presented information is for commercial devices, now available on the market.

Table 1: Batteries and Supercapacitors Unit Characteristics

| Reference | Battery A Li-ion | Battery B Li-ion | Battery C NiMH | SC |
|---|---|---|---|---|
| Type | TS-LFP40AHA | TS-LFP90AHA | VH Module VH F 10S | PC2500 |
| Manufacturer | Thunder Sky | Thunder Sky | Saft | Maxwell |
| Weight (kg) | 1.5 | 3.2 | 3 | 0.725 |
| Volume (L) | 1 | 2.17 | 1.7 | 0.6 |
| Voltage (V) | 3.2* | 3.2* | 12* | 2.7** |
| Capacity/Capacitance | 40Ah @ 0.3C | 90Ah @ 0.3C | 13.5 Ah @ 2C | 2700 F |
| Specific Power [W] | 384 | 864 | 360 | --- |
| Cost (€) | 78.5 | 135.8 | 137.5 | 24.0 |

* Nominal cell voltage; ** Maximum cell voltage

From (4), one can see that $C_{Bat}$, $C_{SC}$, $X_{Bat}$, $X_{SC}$, $K_{Bat}$, and $K_{SC}$ should be reduced to minimize $C_{Tc}$ cost function. However, there are constraints on reduction of all cost function coefficients.

For constrains on $C_{Bat}$ and $C_{SC}$, it is assumed that the cost of each battery and SC units are fixed and independent of the other coefficients. The constraints on the numbers of unit series, $X_{Bat}$ and $X_{SC}$, are function of the powertrain topology. For the current VEIL project, it is considered for all energy storages a nominal DC-link voltage of 96 V with a limited voltage variation (±10%).

For these considerations and for the selected ESSs, the variation of the constraints $X_{Bat}$ and $X_{SC}$, in order to hold the DC-link voltage, are presented in Table 2.

Table 2: Variation of the Constraints $X_{Bat}$ and $X_{SC}$ for 96 V ± 10%

| Reference | $X_{min}$ | $X_{max}$ | DC-link Voltage variation [V] | 1st approach $X_{Bat}$ and $X_{SC}$ Constraints |
|---|---|---|---|---|
| Battery A | 25 | 35 | 87.5 < Vdc < 105.0 | $X_{Bat} = 30$ |
| Battery B | 25 | 35 | 87.5 < Vdc < 105.0 | $X_{Bat} = 30$ |
| Battery C | 7 | 9 | 90.0 < Vdc < 105.0 | $X_{Bat} = 8$ |
| SC | 32 | 42 | 86.4 < Vdc < 105.0 | $X_{SC} = 37$ |

Constraints on the number of branches paralleled are discussed on the next subsections, because $K_{Bat}$, and $K_{SC}$ variation ranges depend on the EV desired performance (autonomy and dynamic response).

### 4.1.1 Drive Cycles

Given the need for energy to propel an automobile, since there are different types of engines/powertrain it was necessary for test procedures to compare several engines/powertrain with each other. These test procedures are called driving cycles. A driving cycle is a standardised driving pattern, described by means of a speed-time table. Therefore, the speed and the acceleration are known for each point of time and the required mechanical power as a function of time can be determined for each vehicle.

Several driving cycles are used and the typically the world-wide can be divided into three groups: European Driving Cycles; US Driving Cycles and Japanese Driving Cycles. For this work it was considered the official's European Driving Cycles, like ECE 15 and EUDC.

The ECE 15 driving cycle represents a typical big city urban driving. It is characterised by low vehicle speed (max. 50 km/h), perfectly adapted to the chosen vehicle type that is limited to 45 km/h, by law. The EUDC cycle describes a suburban route. At the end of the cycle the vehicle accelerates to highway-speed. Both speed and acceleration are higher than in ECE 15. The EUDCL is a suburban cycle for low-powered vehicles. It is similar to the EUDC but the maximum speed is 90 km/h. And, finally, the NEDC is a combined cycle consisting of four ECE 15 cycles followed by an EUDC or EUDCL cycle. The NEDC is also called the ECE cycle. For the VEIL project the maximum speed of the suburban cycle part was readjusted for a 50 km/h maximum speed. The considered NEDC is presented in the Figure 4.

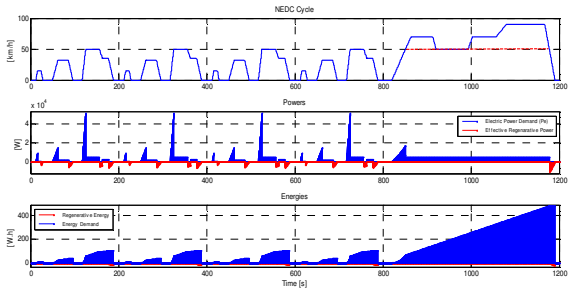


Figure 4: NEDC for low-speed vehicle and NEDC applied to the VEIL speed versus time, and resultant powers and energies.

After modelling the vehicle, taking into account the mechanical parts, including body and transmission units, and the dynamic and aerodynamic vehicle characteristics, with the model used [8][14] applying the chosen driving profile, results were obtained for power and energy demand, and regenerative power and energy, respectively. These results are presented in Figure 4.

Analyzing the power graph shown in Figure 4, we can easily separate the EV demands of high power, low power and the effective regenerative power[1]. The cases of the high and low EV power demands and regenerative power will be analyzed in the next subsections. For the driving cycle analysis, the main interest is the energy required to perform a chosen driven cycle. In other words, this analysis permits to obtain information about the need of energy available in the main energy storage that will define the basic autonomy of the EV, usually the battery banks.

Although the test cycles have different types of requests (e.g. acceleration, maximum speed and braking), as the energy used by SCs is renewable, then in terms of autonomy it is only necessary to assess the number of batteries to use. Therefore, subtracting the effective regenerative energy of the energy demand (Figure 4), we obtain the required energy to move the sample vehicle for the chosen cycle. So, for the modified NEDC (limiting the maximum speed @ 50 km/h), the sample vehicle travel a distance of 9.31 km, with an average speed of 27.94 km/h and require about 1000 Wh.

With the information presented in Figure 4, we can evaluate the minimum number of $K_{Bat}$ for the sample vehicle to achieve one modified NEDC Cycle. The results for each considered battery type are presented in Table 3.

Table 3: Evaluation of the Constraint $K_{Bat}$ for NEDC Cycle

| Reference | $X_{Bat}$ | $K_{Bat}$ | Total energy [kWh] | Modified NEDC Cycle [#x] | Autonomy [km] |
|---|---|---|---|---|---|
| Battery A | 30 | 1 | 3.840 | 3.766 x | 35.0 |
| Battery B | 30 | 1 | 8.640 | 8.474 x | 78.8 |
| Battery C | 8 | 1 | 1.450 | 1.343 x | 12.5 |

As to assure the nominal DC-link voltage of 96 V, there is a minimal number of batteries in series, $X_{Bat}$ (Table 2), the number of modified NEDC cycles possible is bigger than one, for all cases.

[1] Effective Regenerative Power is the power that for the present work can be recovered from the SCs (about 65% of the Total Regenerative Power available on the wheels).

### 4.1.2 Maximum EV Speed Request

For the case of the vehicle cruising at its maximum speed, the power demand is given by:

$$P_{v_{max}} = (\mu_{RR} \cdot m \cdot g) \cdot v_{max} + \left(\frac{1}{2} \cdot \rho \cdot C_D \cdot A_F \cdot v_{max}^2\right) \cdot v_{max} \quad (5)$$

where $P_{v_{max}}$ is the mechanical EV power demand (W) for the maximum speed drive, $\mu_{RR}$ is the coefficient of rolling resistance, $m$ is the considered EV mass (kg), $g$ is the gravity acceleration (9.81 m/s$^2$), $\rho$ represents the air density (1.204 kg/m$^3$ at 20ºC), $C_D$ is the drag coefficient, $A_F$ is the frontal projection area (m$^2$) and $v_{max}$ is the maximum vehicle speed (m/s). In this project and with the aforementioned restrictions the maximum speed considered is 50 km/h on the flat road. In this paper, the EV project vehicle specifications are presented in Table 4, and they were used for this design study.

Table 4: EV Project Vehicle Specifications

| Parameter | Value |
|---|---|
| Vehicle mass (kg) | 500* |
| Rolling Resistance Coefficient | 0.015 |
| Aerodynamic Drag Coefficient | 0.51 |
| Front Area (m$^2$) | 2.4 |
| Wheels radius (m) | 0.26 |
| Gearbox transmission ratio | 10 |

* With the mass of the typical ESSs and 1 passenger.

Computed equation (5), the mechanical EV power demand for the maximum speed drive 50 km/h was 3 kW. Therefore, if it was considered 70% of efficiency of the VEIL full power chain, the electrical power demand is 4.3 kW. Simulation results of the case study are presented in Figure 5.

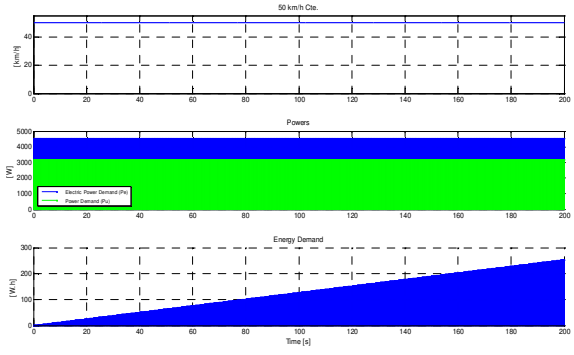


Figure 5: Mechanical, Electrical Power and Energy demands to the VEIL at the constant speed 50 km/h.

When the vehicle cruises at the maximum vehicle speed, are the battery packs alone that provide power to EV due to the limited energy capacity of the other energy systems.

In the previous analysis, this was based on the batteries energy density; now, for the maximum speed, the analysis is made on the specific power of each battery types. The results of this analysis are presented in Table 5.

Table 5: Evaluation of the Constraint $K_{Bat}$ @ 50 km/h

| Reference | $X_{Bat}$ | $K_{Bat}$ | Specific Power [kW] | Autonomy [h] | Autonomy [km] |
|---|---|---|---|---|---|
| Battery A | 30 | 1 | 11.52 | 0.893 | 44.7 |
| Battery B | 30 | 1 | 25.92 | 2.009 | 100.0 |
| Battery C | 8 | 2 | 5.76 | 0.674 | 33.7 |

The $X_{Bat}$ are the presented in Table 2.

### 4.1.3 Acceleration Request

For the case of the acceleration request, during initial phase of each travel, the power demanded by the EV from the powertrain is given by:

$$P_a = \left( \mu_{RR} \cdot m \cdot g + \frac{1}{2} \cdot \rho \cdot C_D \cdot A_F \cdot v^2(t) + M \cdot \frac{dv(t)}{dt} \right) \cdot v(t) \quad (6)$$

where $P_a$ is the EV power demand in (W), and $v(t)$ is the vehicle speed in function of the time (m/s).

The initial acceleration performance for the EV project prototype is defined as accelerating the vehicle from standstill to 50 km/h in 8 s, like to the NEDC cycle, when the vehicle start at standstill to $v_{max}$ (see Figure 4 and 6).

The power demanded by the EV project to achieve the aforementioned acceleration performance was calculated using (6) and is shown in Figure 6. The mechanical EV power demand for the standstill to maximum speed drive 50 km/h was 34.54 kW. Therefore, if it is considered 70% of efficiency of the VEIL power chain, the electrical power demand is 49.35 kW, as can be seen in Figure 6.

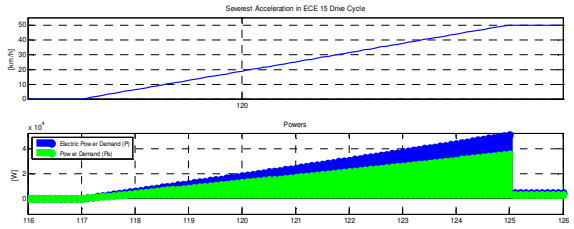


Figure 6: Mechanical and Electrical power demand of the vehicle during the considered severest initial acceleration.

During initial acceleration, both the battery and SC in the EV powertrain have to supply high power to the vehicle. It is evident that if fewer branches in the battery banks (smaller $K_{bat}$) are used, more branches in the SC bank (larger $K_{SC}$) have to be used to meet the vehicle power demand and maintain stable DC-link voltage and vice versa.

For this analysis and for maximum SC power request, let us assume that the batteries provide the power required travelling at maximum speed, cf. 4.1.2, and we need only that the SC give the difference to the acceleration EV power requirement. In this case, we need a 45 kW for 8 s, which is 360 kJ. The system will normally operate at 96 V ± 10% and, we assume for this application, it will be operating at or near its nominal voltage most of time. Dividing the nominal voltage by the nominal cell voltage to get the required number of cells in series, like in 4.1, and $X_{SC}$ = 37 cells. For other hand, the SC current average ($i_a$) is given by:

$$i_a = \left( \frac{P_{SC}}{V_{\min}} + \frac{P_{SC}}{V_{\max}} \right) \Big/ 2 \quad (7)$$

where $P_{SC}$ is the requested power to SCs, and $V_{\min}$ and $V_{\max}$ are, namely, the minimum and maximum SC voltages system. Thus, $i_a$ was calculated to be 474.3 A. The cell resistance for the chosen SC, $R_{cell}$, is 1 mΩ, and the RC time constant is the product of its capacitance value and resistance value. For this example, time constant of one SC is 2.7 s, therefore, the total stack resistance ($R_{total}$) is SC time constant (2.7 s) divided by the total capacitance of the SC system ($C_{total}$). Having all the variables defined to compute the voltage drop ($dV$) during the discharge of the capacitors (8),

$$dV = i_a \cdot \left( \frac{dt}{C_{total}} + R_{total} \right) \quad (8)$$

we will rearrange (8) and solve for $C_{total}$, resulting $C_{total}$ = 264.32 F. Now, with the total value of SC system capacitance and the number of series cells required ($X_{SC}$ = 37 cells) and the expression (9), we can calculate the number of parallel ($K_{SC}$).

$$C_{total} = C_{cell} \cdot \frac{K_{SC}}{X_{SC}} \quad (9)$$

The value of $K_{SC}$ was calculated to be 3.62, and it is assumed $K_{SC}$ = 4.

For other value of the SC power request, namely, if lower SC power is required, decreasing $K_{SC}$ and increasing the supply of power by batteries, we have other configurations of $K_{Bat}$ and $K_{SC}$, such as those presented in Table 6.

Table 6: Evaluation of the Constraints $K_{Bat}$ and $K_{SC}$ for acceleration request

| Combination | Reference | $X_{Bat}$ | $K_{Bat}$ | Specific Power [kW] |
|---|---|---|---|---|
| A | Battery A | 30 | 1 | 11.52 |
| B | Battery B | 30 | 1 | 25.92 |
| C | Battery C | 8 | 2 | 5.76 |
| D | Minimum battery power required | | | 4.30 |
| | | $X_{SC}$ | $K_{SC}$ | Capacitance [F] |
| A | SC | 37 | 3 | 218.92 |
| B | SC | 37 | 2 | 145.95 |
| C | SC | 37 | 4 | 291.90 |
| D | SC | 37 | 4 | 291.90 |

Analyzing the values of $K_{SC}$ shown in Table 6, it is clear that if the batteries specific power is greater, the number of parallels of SCs ($K_{SC}$) decreases. Owner, this is not linear: even a rise of 4.5 times the specific power of batteries (case B), the number of necessary parallel SC is only halved.

### 4.1.4 Energy Regeneration request

In this case, when the EV brake, it is possible to use regenerative energy because the $P_{dem}$ becomes zero and the motor torque becomes negative and thus enables the energy generation. In this case, the most demanding braking NEDC cycle define the minimum value of the SC capacity necessary for the sample vehicle recovered the all braking energy. The representation of the power produced during braking and the effective regenerative power that can actually be stored (considering an energy return path with efficiency of 65%) are shown in Figure 7. Applying the expression (6), suitably adapted to the case of a deceleration of 50 km/h to standstill in 13 s, the total power that can be stored is 10.7 kW, as presented in Figure 7.

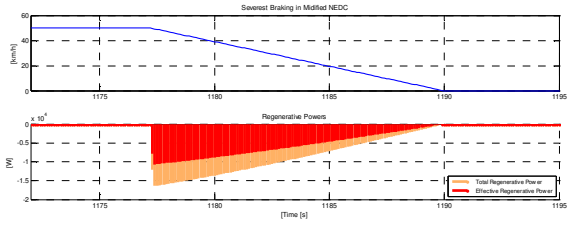


Figure 7: Total and Effective regenerative power of the vehicle during the considered severest breaking phase.

Applying the same approach as in the previous section, expressions (7), (8) and (9), we can to calculate the value of the SC total capacity required in this phase, $C_{total}$ = 91 F, giving a $K_{SC}$ to 1.34, then rounded to the higher integer, $K_{SC}$ = 2. This value is the lower limit of the restriction $K_{SC}$, if we want to store all of the regenerative energy in the more demanding braking NEDC modified cycle.

### 4.1.5 Gradeability Request

The vehicle power demand during grading (Pg) is given as:

$$P_g = \left( \mu_{RR} \cdot m \cdot g + \frac{1}{2} \cdot \rho \cdot C_D \cdot A_F \cdot v_g + M \cdot g \cdot \sin(\theta) \right) \cdot v_g \quad (10)$$

where $\theta$ is the climbing angle and $v_g$ is the maximum request vehicle speed at grading periods.

In this paper, gradeability for the VEIL project vehicle is defined as the ability to grade a road with a climbing angle 6º, which is about 10% inclination at a constant speed of 23.5 km/h.

The first two terms of (10) do not depend on the inclination, but they are function of the minimum power need to put a vehicle in motion. The first term is related to the rolling resistance force and the second is related to the aerodynamic drag force. Considered, when the vehicle is climbing, that its speed is low, the term with greater impact on the power demand is the third term, which is linked to the inclination of the road.

Using (10), the defined gradeability and specifications of the vehicle, presented in Table 4, the power demanded by the vehicle during grading was calculated to be about 4 kW. It should be noticed that around 0.7 kW is from the rolling resistance force and the aerodynamical drag force, and the net power demand for the grading is 3.35 kW. Considering again 70% of the efficiency of the VEIL power chain, the electrical power demand is 5.75 kW for the considered gradeability.

The graphs of power demanded by the EV project to achieve the aforementioned climbing performance are shown in Figure 8.

During grading, only the battery provides power to the vehicle. This is because the supercapacitor has limited energy capacity and cannot be used to power the vehicle during long periods of grading. Therefore, the power supplied by the battery banks is about 5.75 kW, and the power supplied by the supercapacitor bank is zero. Since the supercapacitor does not provide power to the vehicle during grading, gradeability does not constrain $K_{SC}$, but constrains $K_{Bat}$.

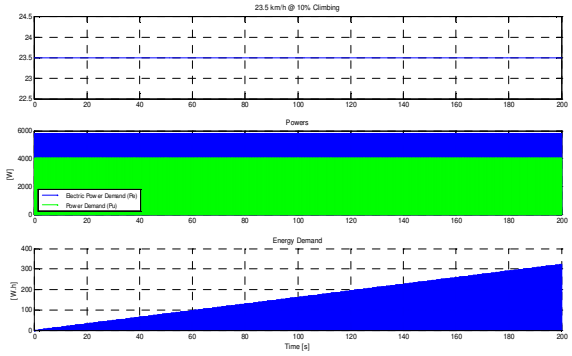


Figure 8 – Power demand to achieve the defined climbing.

Again, the discussion of constraint $K_{Bat}$ is based on the value of the specific power of batteries pre-selected. The results of this analysis are presented in Table 7.

Table 7: Evaluation of the Constraint $K_{Bat}$ @ considered gradeability

| Reference | $X_{Bat}$ | $K_{Bat}$ | Specific Power [kW] | Autonomy [h] | Autonomy [km] |
|---|---|---|---|---|---|
| Battery A | 30 | 1 | 11.52 | 0.67 | 15.70 |
| Battery B | 30 | 1 | 25.92 | 1.5 | 35.25 |
| Battery C | 8 | 2 | 5.76 | 0.5 | 11.75 |

The $X_{Bat}$ are the presented in Table 2.

### 4.1.6 Synopsis of the constraints $K_{Bat}$ and $K_{SC}$

In the previous sections, it were studied the constraints $K_{Bat}$ and $K_{SC}$ for different sample

vehicle operations. The minimum values of the constraints $K_{Bat}$ and $K_{SC}$ resulting of these analyses are presented in Table 8.

Table 8: Constraints $K_{Bat}$ and $K_{SC}$

| Constraints | | | |
|---|---|---|---|
| Battery | | | SC |
| $K_{Bat}$ | | | $K_{SC}$ |
| Battery A | 1 | | 3 [2] |
| Battery B | 1 | | 2 |
| Battery C | 2 | | 4 [3] |

To store all of regenerative energy, the minimum is $K_{SC}$ = 2, possible only for the case of type B battery. In the other cases, $K_{SC}$ must be greater, depending on the value of specific battery power of A and C type; in case C, the need to place a minimum of $K_{SC}$ = 4, is setting the value of $K_{bat}$ in the minimum amount required for a cruising speed of 50 km/h. Somehow, what will define the balance between these constraints is the cost and the weight of the ESSs, as will be analyzed further on.

## 4.2 Backup Energy Supply (PV array) Design

The backup energy system, photovoltaic panels or cells, also can be connected in series to form a branch and multiple branches are paralleled to form a PV array. Therefore, the total cost ($C_{Tb}$) of the PV array system is given by the unit cost ($C_{PV}$) of the number of the series units ($X_{pv}$) and parallel branches ($K_{pv}$) of the PVs, as presented in (11). The costs $C_{Tb}$, and $C_{PV}$ are in European Currency (Euro, €).

$$C_{T_b} = C_{PV} \cdot X_{pv_i} \cdot K_{pv_n} \quad (11)$$

The sample photovoltaic panels used in this work are modules (BP MSX 30) designed for applications requiring a combination of light weight, compactness, and ruggedness. Its unit cost and specific characteristics are presented in Table 9. The presented information is for a commercial device, now available in the electrical market.

Table 9: Characteristics of PV panels

| PV Array | Warranted Power [W] | Voltage [V] | Dimensions L x W [mm] | Mass [Kg] | Cost [€] |
|---|---|---|---|---|---|
| BP MSX 30 | 27 | 16.8-21 | 616 x 495 | 3 | 240 |

The constraint $X_{pv}$ is limited by the DC-link voltage and for its considered value and commercial PV, the constraint $X_{pv}$ was calculated to be 5. But, the number of PV to make the array is function of the dimension of the VEIL rooftop and the hood (the hinged cover over the motor vehicles that allows access to the motor compartment for maintenance and repair), and of the considered PV commercial model. The usable space on the rooftop of the considered vehicle is defined by a surface about 1300 x 1100 mm, and the hood space defined by 550 x 1100 mm. With this dimension it is possible to implant 5 selected PVs, 4 in the rooftop and 1 in the hood, as it is presented in Figure 9.

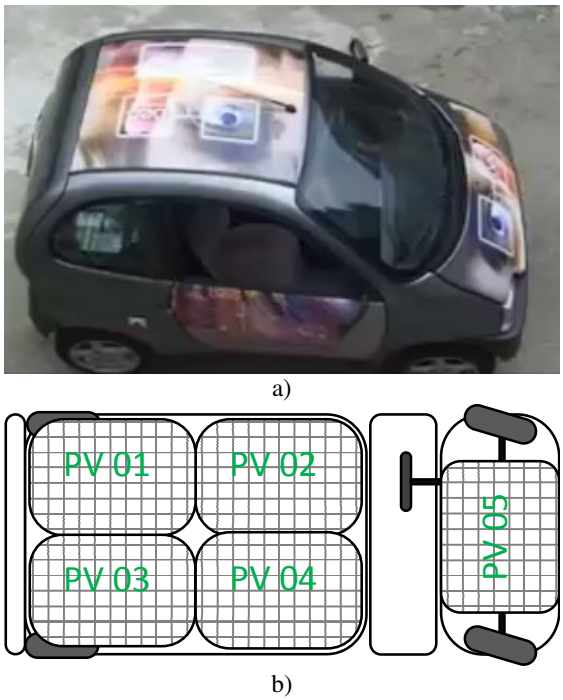


a)

b)

Figure 9: a) View from the top of VEIL project; b) Schema of the PV array implementation.

As there is not usable space in the VEIL vehicle to get more PV panels, we find that the $X_{pv}$ and $K_{pv}$ may have the values, 5 and 1, respectively. Thus, the total cost of the PV array will have only two values, zero cost is without the support of renewable energy or a fixed cost of 1200 €. The same approach can be made for the weight (0 or 15 kg).

For the solar energy, the study uses the average hourly statistics for direct normal solar radiation [Wh/m²] – for the last 30 years at the project location, Coimbra (see Figure 10). As an example, for a typical day of two different months, November and August, with the minimum and maximum solar radiation, respectively, and using the efficiency PV array model, it can be computed the global generated energy by the panels, as shown in Figure 11, and considering, somehow, the mounting position of the PV panels

[2] For $K_{Bat}$ considered. If $K_{Bat}$ increases, $K_{SC}$ can decrease to a minimum of 2.

[3] For $K_{Bat}$ considered. If $K_{Bat}$ increases, $K_{SC}$ can decrease to a minimum of 2.

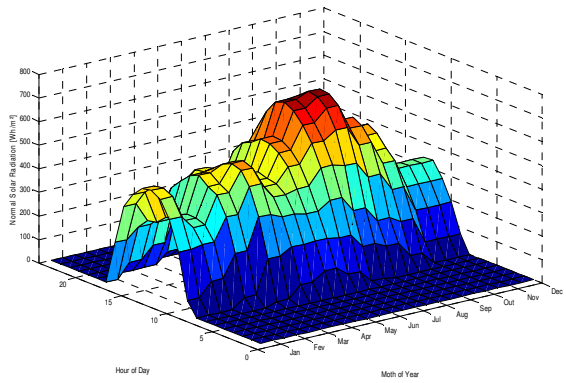


Figure 10: Average hourly normal solar radiation.

In Figure 11, we can see that the variation of the energy accumulated during the typical day of the considered two months, is positioned between the 900 Wh and 1350 Wh a day. With these results, the advantage of this topology PV array investment is the recovering of at least 900 Wh a day, when the car is at direct sunlight. Next it needs to review the weight of the increased number of branches in parallel to batteries versus investing in this backup system.

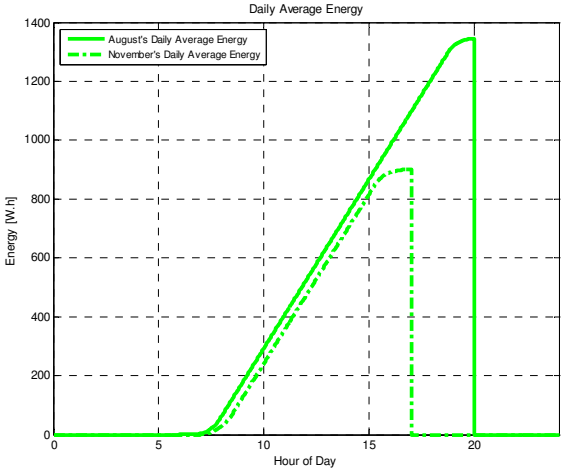


Figure 11: Daily average energy for typical months.

## 4.3 Cost Reduction by Constraints $K_{Bat}$ and $K_{SC}$

To analyze the cost reduction with the previous study of constrains, for example, we can use a hypothetic scenario, where there were considered three different time periods: a first displacement in the morning, starting at 7:30 am and taking 1.5 h (to get to work, for instance), a second period where the car is parked outdoor and lasting 8 h, and a third period equal to the first one, corresponding to the return back home, from 17:00 to 18:30 pm. To fulfil the 1.5 h travel in the morning and in the evening, based on NEDC cycle, we need to use 4.5 NEDCs, totalizing 40.24 km, followed by 8 h parked and again 4.5 NEDCs. The total journey distance is about 80.48 km. For this approach it is needed to include an additional restriction (12), where the total energy needed ($W_{Totalmin}$) for to accomplish the considered number of considered cycle test, is given by:

$$W_{Total} \geq N° Cycle \cdot W_{NEDC} \quad (12)$$

where $W_{Total}$ is the sum of the total energy of the battery banks, the total regenerative energy in all studied cycle tests and the minimum energy recovered by the PV array, and it is given by (13):

$$W_{Total_{\min}} = K_{bat} \cdot W_{bat/k_{bat}} + N° Cycle \cdot W_{reg/cycle} + K_{PV} \cdot W_{PV/k_{PV}} \quad (13)$$

For this example the minimum energy needed in each NEDC cycle is about 1000 Wh.

Applying the constraint (13) together with the restrictions listed previously, cf. 4.1.6, we see that minimizing the cost of storage systems for energy, depending on the different types of batteries, get the results shown in Table 10.

Table 10: Evaluation of the Total Costs for 9 NEDCs

| Reference | $X_{Bat}$ | $K_{Bat}$ | $X_{SC}$ | $K_{SC}$ | $X_{PV}$ | $K_{PV}$ | Total Cost [€] | Weight [kg] | Expected Autonomy [km] |
|---|---|---|---|---|---|---|---|---|---|
| Battery A | 30 | **2** | 37 | **3** | 5 | **0** | 7374 | 170.48 | 81.3 |
| Battery B | 30 | **1** | 37 | **2** | 5 | **0** | 5850 | 149.65 | 90.1 |
| Battery C | 8 | **6** | 37 | **3** | 5 | **0** | 9264 | 224.48 | 90.6 |

From Table 10, it can be seen that the most viable option, both for cost and weight to the presented scenario, is to use the battery type B, because it will minimize the use of SC. So with a single bank of batteries of the type B and 2 banks of SCs, we can make the outward journey and return. The other options are more expensive and heavier, and the solution with the same chemical in the solution B is better than the solution with the NiMH batteries. The only solution which could consider the use of PV is a solution with batteries of type C, it can reduce the number of banks of batteries to use up 5 and the PV array, although this brings an increase in initial cost of investment, plus a minimization of the cost of energy purchased for loads of storage systems for energy.

The same approach can be made for other scenarios, including a scenario corresponding to a typical routine for mobility in big European cities, with low average speed and very frequent stops and goes. To simulate this behaviour it was used the ECE 15 cycle, presented in Figure 4 (first 200s). The travel in the morning is constituted by a sequence of 27 ECE 15 cycles, corresponding to nearly 27.35 km. The same distance has to be travelled in the evening to make the way back. This scenario consists then in 27 ECE 15 cycles during 1.5 h, followed by a period of 8 h parked

outdoor, and then again 27 ECE cycles. The total journey distance is 54.7 km (2 times 27.35 km). The results are presented in the Table 11.

Table 11: Evaluation of the Total Costs for 27 ECEs

| Reference | $X_{Bat}$ | $K_{Bat}$ | $X_{SC}$ | $K_{SC}$ | $X_{PV}$ | $K_{PV}$ | Total Cost [€] | Weight [kg] | Expected Autonomy [km] |
|---|---|---|---|---|---|---|---|---|---|
| Battery A | 30 | **2** | 37 | **3** | 5 | **0** | 7374 | 170.48 | 61.6 |
| Battery B | 30 | **1** | 37 | **2** | 5 | **0** | 5850 | 149.65 | 68.6 |
| Battery C | 8 | **5** | 37 | **3** | 5 | **0** | 8134 | 200.48 | 58.5 |

The results presented in Table 11, also notes that, for the proposed scenario, the more feasible option is to use batteries type B. Also, in this scenario, the use of solar energy is not a viable solution in terms of investment, compared to other considered solutions. We conclude that the same configuration based on 1 bank of batteries type B and 2 banks of SCS, allows both the first and the second considered scenario.

Finally, a third scenario corresponds to an extra urban utilization at the VEIL full speed that for this kind of vehicle is limited to 45 km/h. Nevertheless, the study was done considering the slightly higher speed of 50 km/h, as in Figure 8. In this case, 1.5 h allows to cover a 73.59 km distance between home and work in the morning and the same distance in the evening, to return back home (almost 149.18 km, in total). The results are presented in the Table 12.

Table 12: Evaluation of the Total Costs @ 50 km/h for 2 periods of 1.5 h

| Reference | $X_{Bat}$ | $K_{Bat}$ | $X_{SC}$ | $K_{SC}$ | $X_{PV}$ | $K_{PV}$ | Total Cost [k€] | Weight [kg] | Expected Autonomy [km] |
|---|---|---|---|---|---|---|---|---|---|
| Battery A | 30 | **4** | 37 | **2** | 5 | **0** | 11.2 | 233.65 | 178.8 |
| Battery B | 30 | **2** | 37 | **2** | 5 | **0** | 9.92 | 245.65 | 201.2 |
| Battery C | 8 | **10** | 37 | **2** | 5 | **0** | 12.78 | 293.65 | 168.8 |

For this scenario, as expected, it is needed greater energy to perform the path-way plus the way back. However, it is concluded that the best solution is still based on the batteries type B, there is only need to insert one more bank to increase the autonomy and achieve the desired trip. This gives us clues to the possibility, in the future, to exist modular systems of energy storages configurable by the user's request.

Therefore, the results of the proposed configurations were based on 500 kg weight of the VEIL Thus there is interest on verifying by simulation if the proposed design and the influence of the weight of the storage systems does not significantly affect the performance of the vehicle. Simulation

Based on the results for the different designs obtained through the methodology previously presented, can be made comparative simulations of the various options proposed. These simulations are made using the VEIL dynamical model, with the different weights (Tables 10, 11 and 12) of considered energy storages[4], and the three presented different scenarios for typical driving cycles, were computed using Matlab/Simulink®, provided with the SimPowerSystems library [14]. The results, namely the daily average energy evolution, for the three considered scenario are presented in Figure 12, 13 and 14.

For Figure 12, it can conclude that the presented solutions based on the B and C-type batteries, achieve the journey request, but the solution with batteries A, not. It appears that the development of solutions B and C is very similar. It is noted that in the case of A-type batteries, taking into account the weight of the designed systems, the vehicle has not the energy needed to do the full journey trip. However, if it is inserted the backup system (PV Array), recovering the solar energy, when the vehicle is parked, this allows to do his way back.

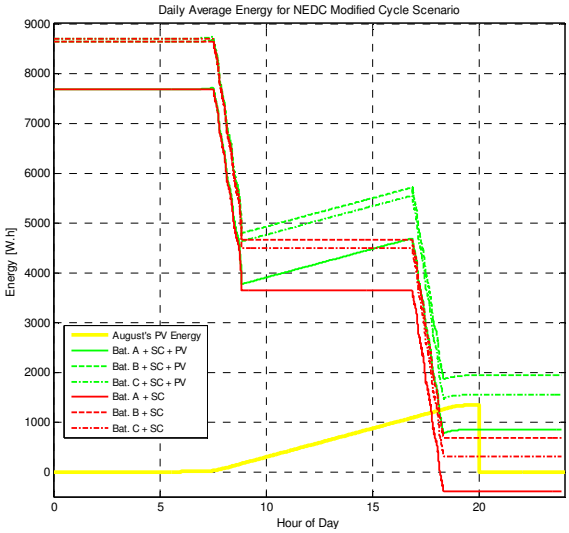


Figure 12: Daily Average Energy for NEDC Modified Cycle Scenario.

For ECE 15 Cycle Scenario (see Figure 13), analyzing the curves of the daily average energies, they show that the SCs are very important in this scenario, because the circuit has a higher number of acceleration and braking. All designed situations reached the objectives of the scenarios outlined. The situation based on the B-type battery shows that it is the option that offer more autonomy and allow without problems making these first two scenarios.

[4] It was considered a 3 kg weight increase for each necessary SCs and PV array DC/DC converters.

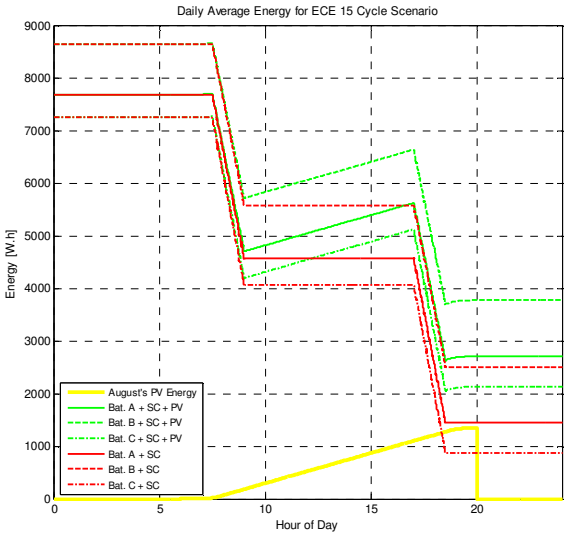


Figure 13: Daily Average Energy for ECE 15 Cycle Scenario.

When the vehicle cruises at the maximum vehicle speed during the stipulated 2 periods of 1.5 hours, it can be conclude that, unless an increase of energy necessary to carry out these trips, the behaviour of the 3 cases studied is identical to previous scenarios, showing again, the option with the B type batteries, is the most indicated. However, it is seen that in the case of C-type batteries, it can not make the specified journey back but that the help of the PV array is enough to end this trip.

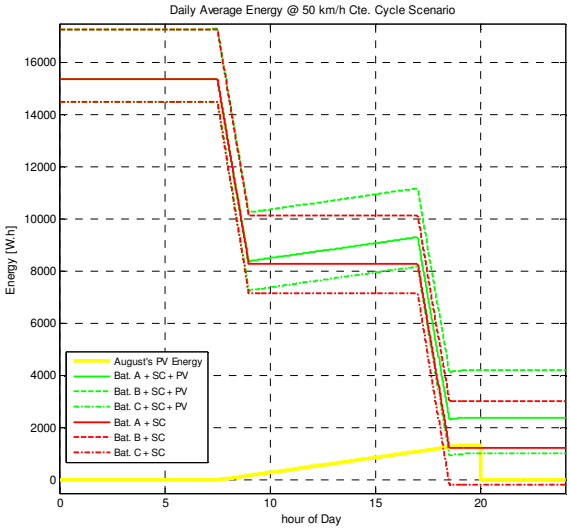


Figure 14: Daily Average Energy @ 50 km/h Cte. Cycle Scenario.

From all presented results, it is shown that the use of a backup system based on solar energy, can be a good means to recharge the batteries, allowing in some cases to deal with unexpected routes and especially minimize the need of full recharge of the ESSs through the power network during the night. It is also important to compensate the batteries self discharged when parked outside, without the possibility to plug to an electric power source, for long periods.

# 5 Conclusions

This work presents a complete methodology to optimize the sizing of the ESSs for an EV. As an example, it was used the ISEC EV VEIL project [7][15] from three considered driving cycles, specified maximum speed, acceleration performance, regenerative energy and gradeability requests. Some simulation results of multiple energy sources hybridization were presented, considering different ESSs and different scenarios for the small presented EV. The emphasis of this work is the comparative study on the impact of different ESSs utilization, namely different combinations of the considered sources, versus the different scenarios for daily use. It should be clearly stated that the presented results depend strongly on the ESSs price, weight, energy and power, and may change as these characteristics modify.

The complete methodology is fast, objective, and quite accurate, since the simulations obtained for the proposed designs are within the minimum request results. It was also studied the possibility of using a backup system based on solar energy, that may be considered in the design, or as an extra to cope with unforeseen routines and to minimize the recharge of ESSs through the power network. The methodology can be improved by inclusion of techniques for multi-objective optimization, minimizing the initial cost, the cost of the ESSs recharges, and weight, maximizing the autonomy and life cycle of ESSs. This type of study is important for the correct sizing of the ESSs, depending on the intended uses of an EV, in order to maximize the autonomy and the performance with a minimum initial cost and utilization costs.

# References

[1] IEA, *World Energy Outlook 2004*, OCDE, pp.58, 2004.

[2] IEA, *Key World Energy Statistics*, 2006 edition.

[3] N. Künzli, R. Kaiser, S. Medina, et al., *Public-health impact of outdoor and traffic-related air pollution: a European assessment*, The Lancet, vol. 356, Issue 9232, pp. 795-801, Sept. 2000.

[4] L. Int Panis, R. Torfs, *Health effects of traffic related air pollution*, European Ele-Drive

Transportation Conference (EET-2007), Conf. Proc., 30th May - 1st Jun. 2007.

[5] P.G. Pereirinha, J.C. Quadrado, J. Esteves, *Sustainable Mobility: Part II – Some Possible Solutions Using Electric and Hybrid Vehicles*, 1st Inter. Conf. on Electrical Engineering (CEE´05), Conf. Proc., Oct. 2005.

[6] R. Gremban, *PHEVs: the Technical Side*, European Ele-Drive Transportation Conference (EET-2007), Conf. Proc., May/Jun. 2007.

[7] P. G. Pereirinha, J. Trovão et al, *The Electric Vehicle VEIL Project: A Modular Platform for Research and Education*, European Ele-Drive Transportation Conference (EET-2007), Conf. Proc., May/Jun. 2007.

[8] Paulo G. Pereirinha, João P. Trovão, *Comparative study of multiple energy sources utilization in a small electric vehicle*, European Ele-Drive Transportation Conference (EET-2008), Conf. Proc., Mar. 11-13, 2008.

[9] K.T. Chau, Y.S. Wong, *Hybridization of energy sources in electric vehicles*, Energy Convers Mgmt 42 – 9, pp. 1059-1069, 2001.

[10] R. Schupbach , J. Balda , M. Zolot and B. Kramer, *Design methodology of a combined battery–ultracapacitor energy storage unit for vehicle power management*, Proc. IEEE Power Electron. Spec. Conf. (PESC'03), Acapulco, Mexico, 2003, p. 88.

[11] Wu, Y.; Gao, H., *Optimization of Fuel Cell and Supercapacitor for Fuel-Cell Electric Vehicles*, IEEE Trans. on Veh. Technol., Vol. 55, No. 6, Nov. 2006, pp. 1748-1755.

[12] R. Schupbach and J. Balda *The role of ultracapacitors in an energy storage unit for vehicle power management*, Proc. IEEE Veh. Technol. Conf., Orlando, FL, 2003, p. 3236.

[13] W. Gao, *Performance comparison of a fuel cell-battery hybrid powertrain and a fuel cell–ultracapacitor hybrid powertrain*, IEEE Trans. Veh. Technol., vol. 54, pp. 846, May 2005.

[14] João P. Trovão, Paulo G. Pereirinha, Fernando J. T. E. Ferreira, *Comparative Study of Different Electric Machines in the Powertrain of a Small Electric Vehicle*, 18th International Conference on Electrical Machines (ICEM'08), Vilamoura, Portugal, 6-9 Sept. 2008.

[15] Paulo G. Pereirinha, João P. Trovão, L. Marques, M. Silva, J. Silvestre, F. Santos, *Advances in the Electric Vehicle Project-VEIL Used as a Modular Platform for Research and Education*, EVS24 International Battery, Hybrid and Fuel Cell Electric Vehicle Symposium, Stavanger, Norway, 13-16 May 2009.

# Authors

João Pedro F. Trovão received the Electrical Engineering degree in 1999 and the MSc degree in Electrical Engineering – Power System in 2004, from the Coimbra University, Portugal. Currently he is teaching at the Electrical Engineering Department of the Engineering Institute of Coimbra (DEE-ISEC) and he is preparing his Ph.D. degree. His teaching and research interests cover the areas of electric drives, renewable energy, power quality and rotating electrical machines.

Paulo G. Pereirinha obtained his PhD in Electrical Engineering from the Coimbra University, Portugal. Full-time Assistant from 1995, Eq. Adjunct Professor from 1997 and Coordinator Professor since 2009 at the Electrical Engineering Department of the Engineering Institute of Coimbra (DEE-ISEC). His classes and research interest includes electrical machines, electric vehicles, finite elements and renewable energies. He is a founding member of the Portuguese Electric Vehicle Association and member of its administration board. Member of the Portuguese Electrotec. Normalisation Technical Committee, CTE 69 – Electrical Systems for Electrical Road Vehicles.

H. Jorge – received his Electrical Engineering degree in 1985 and his PhD degree in 1999, both from the University of Coimbra. He is Auxiliary Professor at the Department of Electrical Engineering of University of Coimbra. His teaching and research interests include power systems, load research, load forecast, load profile, power quality, power distribution, energy efficiency and energy storage. He is an IEEE member since 1992.